

ade 950 531

(12)

AD-A141 343



TECHNICAL REPORT RR-CR-84-1

10.0 micrometer
10.0 μm GRADIENT INDEX OPTICAL COMPONENT DESIGN

Duncan T. Moore
Gradient Lens Corporation
P. O. Box 5053
River Campus Station
Rochester, NY 14627

NOVEMBER 1983

Approved for public release; distribution unlimited.



U.S. ARMY MISSILE COMMAND

Redstone Arsenal, Alabama 35896

DTIC FILE COPY

Prepared for
Research Directorate
US Army Missile Laboratory

DTIC
ELECTE
MAY 14 1984
S
A
D

SEE FORM 287, 1 NOV 83 PREVIOUS EDITION MAY BE USED

B4 05 14 055

DISPOSITION INSTRUCTIONS

**DESTROY THIS REPORT WHEN IT IS NO LONGER NEEDED. DO NOT
RETURN IT TO THE ORIGINATOR.**

DISCLAIMER

**THE FINDINGS IN THIS REPORT ARE NOT TO BE CONSTRUED AS AN
OFFICIAL DEPARTMENT OF THE ARMY POSITION UNLESS SO DESIGNATED
BY OTHER AUTHORIZED DOCUMENTS.**

TRADE NAMES

**USE OF TRADE NAMES OR MANUFACTURERS IN THIS REPORT DOES
NOT CONSTITUTE AN OFFICIAL INDORSEMENT OR APPROVAL OF
THE USE OF SUCH COMMERCIAL HARDWARE OR SOFTWARE.**

UNCLASSIFIED

SECURITY CLASSIFICATION OF THIS PAGE (When Data Entered)

REPORT DOCUMENTATION PAGE		READ INSTRUCTIONS BEFORE COMPLETING FORM
1. REPORT NUMBER RR-CR-84-1	2. GOVT ACCESSION NO. ADA141 343	3. RECIPIENT'S CATALOG NUMBER
4. TITLE (and Subtitle) 10.6 μ m GRADIENT INDEX OPTICAL COMPONENT DESIGN		5. TYPE OF REPORT & PERIOD COVERED
		6. PERFORMING ORG. REPORT NUMBER
7. AUTHOR(s) Duncan T. Moore		8. CONTRACT OR GRANT NUMBER(s)
9. PERFORMING ORGANIZATION NAME AND ADDRESS Gradient Lens Corporation P. O. Box 5053, River Campus Station Rochester, NY 14627		10. PROGRAM ELEMENT, PROJECT, TASK AREA & WORK UNIT NUMBERS
11. CONTROLLING OFFICE NAME AND ADDRESS Commander, US Army Missile Command ATTN: DRSMI-RPT Redstone Arsenal, AL 35898		12. REPORT DATE November 1983
		13. NUMBER OF PAGES 17
14. MONITORING AGENCY NAME & ADDRESS (if different from Controlling Office)		15. SECURITY CLASS. (of this report) Unclassified
		15a. DECLASSIFICATION/DOWNGRADING SCHEDULE
16. DISTRIBUTION STATEMENT (of this Report) Approved for public release; distribution unlimited.		
17. DISTRIBUTION STATEMENT (of the abstract entered in Block 20, if different from Report)		
18. SUPPLEMENTARY NOTES		
19. KEY WORDS (Continue on reverse side if necessary and identify by block number) Gradient index Zinc Sulfide Zinc Selenide Lenses Optical design		
20. ABSTRACT (Continue on reverse side if necessary and identify by block number) Testing methods needed to determine the optical characteristics of zinc selenide and zinc sulfide gradient index materials are evaluated. The methods described include measurements for homogeneity of the material, transmission and regularity of the profile. In addition, the physical properties (i.e., the concentration of selenium and sulphur versus the spatial coordinate) are described.		

(continued)

UNCLASSIFIED

SECURITY CLASSIFICATION OF THIS PAGE(When Data Entered)

Three designs have been conducted to show the profile that is needed for axial and radial gradient lenses fabricated from zinc selenide and zinc sulfide. The problem of correcting the aberrations of an ogive surface are described and possible solutions to this problem are outlined. (author)

↓
a. variations

UNCLASSIFIED

SECURITY CLASSIFICATION OF THIS PAGE(When Data Entered)

CONTENTS

	Page
I. INTRODUCTION.	3
II. TESTING METHODS	7
III. DESIGN OF 10.6 MICROMETER OPTICAL COMPONENTS.	7
IV. REQUIREMENTS OF AN AXIAL GRADIENT LENS BLANK.	8
V. REQUIREMENTS OF A RADIAL GRADIENT SINGLE ELEMENT BLANK.	10
VI. DESIGN OF AN OGIVE CORRECTOR PLATE.	11
REFERENCES	16

Accession For	
NEIS GRA&I	<input checked="" type="checkbox"/>
ERIC TAB	<input type="checkbox"/>
Announced	<input type="checkbox"/>
Certification	
Distribution/	
Availability Codes	
Dist	Avail and/or Special
A-1	



I. INTRODUCTION

Four optical properties must be measured in order to adequately characterize zinc selenide/zinc sulfide gradient index materials: (1) the transmission of the material, (2) the base index of refraction, (3) the index of refraction profile (variation of index of refraction with spatial coordinate), and (4) the uniformity of the gradient. In addition, one physical property (the concentration of selenium and/or sulfur as a function of position) must be measured. This latter measurement is necessary at the laboratory stages to adequately describe the physical model which will eventually predict the index of refraction from compositional information.

While it is expected that the transmission of zinc selenide/zinc sulfide gradient index materials will have transmission properties given by the average of the sulfide and selenide independently, it is necessary to verify this. For example, the transmission of a sample which has 50 percent zinc selenide and 50 percent zinc sulfide at a certain point is expected to have the average transmittance of the two materials at that particular wavelength. However, because the combination materials cannot be deposited at the optimum rates, this combination is expected to have a somewhat lower transmission than this average. (It is well known that the ideal temperatures and pressures for the two materials to create the best materials are not the same. Therefore, at a laboratory level, this transmission must be measured). In addition, a few samples should be manufactured which are not gradient index material but rather simply combinations of the two materials so that the transmission of these can be measured to determine what the optimum conditions are. For example, a series of samples which are homogeneous in nature consisting of approximately 20 percent zinc selenide and 80 percent sulfide, 40;60, 60;40, 80;20, should be manufactured. These will allow for a adequate determination of the transmission of these materials and thus a prediction of the transmission of an index of refraction gradient made of these two compositions.

The system for making such measurements is quite straight-forward and should consist simply of an infrared spectrophotometer. A number of such instruments are commercially manufactured. The measurements should be made between 0.5 micrometers and 12 micrometers. One additional problem may arise concerning the deposit of the gradient. For example, if a series of discrete steps are produced in the material, each with a slightly different index of refraction, then one would expect reflection from each of these boundary layers. This will contribute to an effective loss in transmission which must be separated from the normal transmission errors in the bulk material. Thus, one would expect, in materials where step indices of refraction are used, to get a somewhat lower transmission than would be a continuous variation in index of refraction.

The optical performance of a gradient index component is directly determined by the uniformity of the index of refraction profile; that is, as a function of the aperture coordinate, the profile should be the same along all lines.

However, it is well known in the chemical vapor deposition method of zinc selenide and zinc sulfide that the formation of small nucleation sites results in a deposition of material in a non-uniform way. For example, at a nucleation site, more material will be deposited as a function of time and, thus, a bump will be formed. In the manufacture of homogeneous zinc selenide or zinc sulfide, this is not a problem since the material being deposited is of a uniform composition throughout the entire deposition time. However, since the deposited material is to be changed in a systematic way, once a nucleation site is formed, the bump that results creates a surface of constant index which has small perturbations on it. These perturbations result in wavefront error throughout the material. The effect will be to have a wavefront which will be nominally spherical or plane, with perturbations superimposed upon it. To estimate the errors of these, let us consider the following problem. Suppose, at some point in the material, a nucleation site is formed which has a height above the normal deposition plane of 10 micrometers. After the nucleation site has been formed, the layers deposited above it are plane except for a 10 micrometer bump. This continues until the deposition has been completed. The surface is now polished plane and the last deposited layer will be removed. A part of the index of refraction profile which corresponds to a depth of 10 micrometers is exposed at a point above the nucleation site. If the index of refraction between the area above the nucleation and the normal material is 0.1 the optical path introduced by this effect is 1.0 micrometer (that is, 1/10 of a wave at 10.6 micrometers). If the nucleation site causes a bump of 100 microns, with the same index of refraction variation, then the effect will be to create a one wavelength optical path variation. These local inhomogenities have the same effect as grinding and polishing errors in normal optical fabrication. Thus, they can be interpreted and the tolerances can be determined in the same way that these optical path errors are calculated. In normal optics used for high quality imaging, it is usually necessary to maintain these errors through less than λ by four (i.e., an optical path error of 2.5 micrometers at 10.6). Thus, if the index profile over the depth varies by 0.01 it will be necessary to be sure that the corresponding heights be less than 250 micrometers. Other combinations of nucleation heights and index of refraction are, of course, possible. By reducing the index of refraction difference over the material, particularly near the surface, one can tolerate an increase in the height of these nucleation sites.

The measurement of the index of refraction profile (i.e., the variation in index of refraction as a function of spatial coordinate) can be measured in a number of ways. There are some unique problems in measuring a profile where the materials have a high index of refraction. Because it is possible to generate index of refraction variations of 0.2 in infrared materials (e.g., in zinc selenide or in germanium) over depths of only a few millimeters, the slope of the index of refraction profile can be enormous. For example, an index change of 0.2 over a distance of 1 millimeter creates a slope of 0.2 mm.^{-1} . This should be compared with the gradients manufactured in optical glasses for visible use where a typical index of refraction profile is 0.5 over 5 millimeters. This results in a slope of 0.01 mm.^{-1} . The effect of this is to cause problems with normal interferometric measurement techniques. In these techniques, two surfaces of the material are polished such that the gradient is parallel to the surfaces. Thus, light propagates through the

sample perpendicular to the gradient. The optical path introduced by such a material is given by the product of the thickness of the polished sample and the index of refraction change (Δn). By taking this number and dividing by the wavelength of light, one determines the number of interference fringes that will be observed. For example, if the index change is 0.01 and the sample thickness is 2 millimeters, the optical path in such materials is 20 micrometers. If the wavelength of the instant radiation is 0.05 micrometers, then 40 interference fringes will be seen in a Mach-Zehnder interferometer (80 will be observed in a Twyman-Green configuration). Thus, 40 fringes will be seen over a distance of 5 millimeters (the depth of the gradient) or 8 fringes per millimeter. Now consider an infrared material such as zinc selenide. In this case, the index change can be 0.2. Assuming a sample preparation thickness of 2 millimeters and a depth of 1 millimeter, the optical path in this system is 400 micrometers and, at 10.6 microns, the number of fringes will be 40. Thus, there will be 40 fringes over a thickness of 1 millimeter. This corresponds to a fringe spacing of 25 micrometers which is 2 1/2 times the wavelength of incident radiation. While this is not an unsolvable problem, it does create a high fringe density and requires high performance optics to image the sample onto the detector plane.

Two solutions have been offered for this problem. The first is to use standard interferometric techniques but to introduce a modulation with two frequencies. The system, called a harmonic interferometer, has been described elsewhere [1]. The results of the measurement of a zinc selenide/zinc sulfide combination have been performed on this instrument (see Figure 1). However, in this situation, the sample thickness was reduced to about one-half of a millimeter in order to adequately reduce the fringe density.

The second solution is one which provides an index of refraction measurement by observing polarization changes at the surface. The system, called a phase lock ellipsometer, modulates the input polarization of a beam incident at an angle near the Brewster's angle. The polarization of the light changes. The results are accurate to about 0.01 in the current system. With some improvements, this could be increased to 0.001. This only results, however, in an accuracy of one hundredth of the index variation, whereas interferometric techniques result in measurements of the order of 0.0001 of the index of refraction variation. However, it is not limited in any way by the slope of the profile. The results of measurements of this instrument are shown in Figure 2 [2]. This latter technique suffers from one important effect; that is, it only measures the surface. This is an advantage when there are very thin layers, however, it is susceptible to surface preparation methods and, thus, the use of it to measure absolute index of refraction is somewhat dubious. Since the surface is prepared in the same way, it is expected that this will provide at least an indication of the index of refraction profile in very steep gradients.

The last optical property that needs to be characterized is the base index of refraction. In interferometer methods, only the index of refraction variations are characterized and, thus, one never knows whether the reference index of refraction is 1.5 or 2.5. While one may argue that some point in the material is a baseline (e.g., one could assume that there is a homogeneous composition of zinc selenide to deposit and, thus, the index of

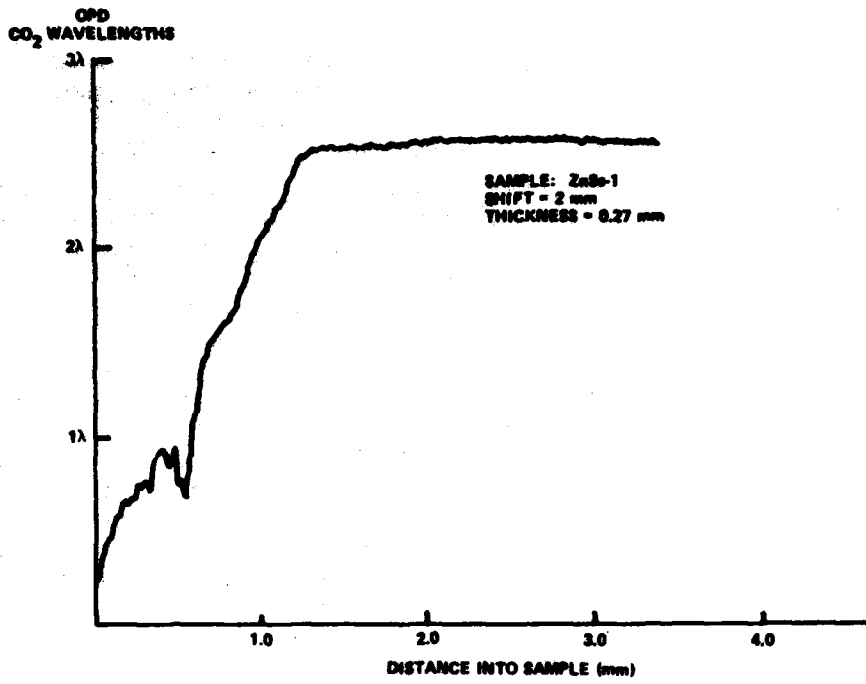


Figure 1. Zinc-Selenide, Sulfide gradient.

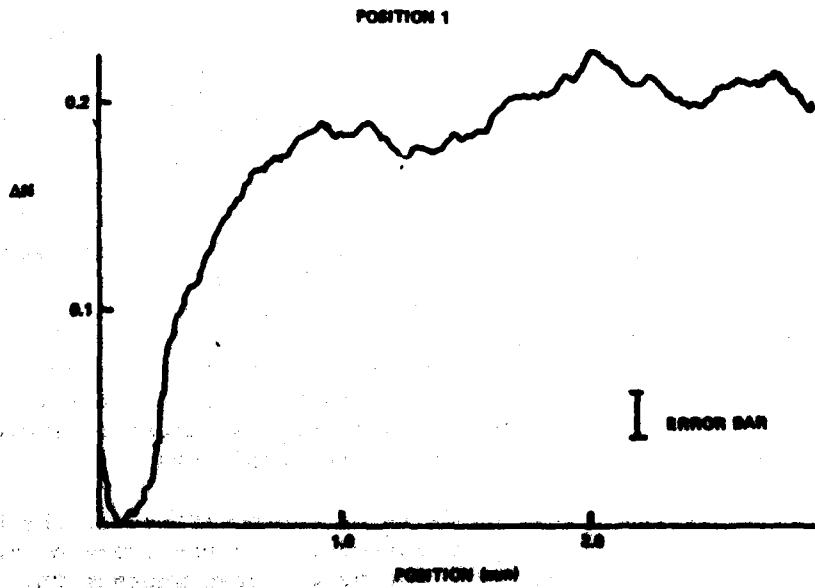


Figure 2. Zinc-Selenide, Sulfide gradient.

refraction is known at that point), this is probably not adequate in normal optical systems. Again, there are two possibilities. One is to use an interferometric technique which measures the absolute index of refraction by measuring the optical path difference as the sample is tilted in one arm of a Mach-Zehnder interferometer. Knowing the thickness of the sample, it can be shown that a measurement of the absolute index of refraction can be made [3]. This measurement is currently available to about 0.001 and is rather independent of the base index of refraction. The second technique is to use the phase lock ellipsometer to make such measurements. Currently such measurements have been made to an accuracy of about 0.05 but they can be improved by an order of magnitude by a change in instrumentation. The two techniques, taken in combination, give adequate results and are well within the needs of the lens design. The index of refraction as a function of wavelength is measured to about 0.005. There currently exists no method by which a company can get these measurements made. Thus, this represents a research topic which must be solved to do gradient index as well as homogeneous optics.

II. TESTING METHODS

One final measurement needs to be made in the laboratory stages. All models which predict the index of refraction of the function of spatial coordinate are based on concentration of the various constituent parts. For example, by knowing the variation of selenium within the material, one should be able to predict the resulting index of refraction profile. This is necessary to the parameters of the lens design, which are normally given in index of refraction versus spatial coordinate, can be translated into materials parameters. In order to correlate these two, it is necessary to measure the concentration of the materials. Thus, one would recommend that microprobe analysis be done on the material to determine this data. There are a number of methods which could be applied. One of them is based on energy dispersive techniques which are well suited to these samples. If the samples are prepared so that the gradient is exposed, as it would be for interferometric techniques, then a scanning electronmicroscope can sample various locations in the gradient and make a compositional measurement. This technique is well known in optics and has been used to measure silver concentrations as a function of depth in optical materials. It may be necessary, in order to give proper correlation, to make as many as 10 to 15 sample measurements. This will assure direct correlation of index of refraction with materials properties.

III. DESIGN OF 10.6 MICROMETER OPTICAL COMPONENTS

Two gradient index lens systems have been designed to specify the type of lens blanks that need to be produced using zinc selenide/zinc sulfide materials. Because an axial gradient and a radial gradient have different effects on the performance of a lens, the exact aberrations that are corrected differ between the two designs. The underlying theme is the determination of the profile of the index of refraction as a function of position in order to write a series of specifications for a chemical vapor deposited zinc selenide/zinc sulfide gradient index material.

IV. REQUIREMENTS OF AN AXIAL GRADIENT LENS BLANK

The design of axial gradient single element lenses corrected for spherical aberration and coma has been described [4]. The important parameters for correcting spherical aberrations are the first curvature of the lens and the value of the first coefficient of the index of refraction profile. If the index of refraction is given by

$$N(z) = N N_{00} + N_{01} z + \dots$$

then the important parameter for aberration correction is the N_{01} coefficient. Further, it has been shown that this coefficient needs to be maintained over distance equal to the sag of the surface (e.g., for a lens of aperture 50 mm and with a first curvature equal to 0.00714 mm^{-1} , then this sag is equal to 2.2 mm). After this distance, the profile may become homogeneous to take on any profile that is suitable to the other production parameters.

A number of single element gradient index components have been designed using a base index of 2.24 corresponding to zinc sulfide and 2.43 corresponding to zinc selenide. It has been assumed that the diameter of the lens is 50 mm. Various focal lengths have been chosen. Table 1 gives a summary of those results including the design parameters, the values of the curvature (cv_1 and cv_2), the gradient depth that needs to be maintained, and the index change (Δn) that needs to be produced. It can be seen that even in the situation where an $f/1$ single lens element is designed, the value of the change of index is only 0.119 (i.e., only one half the capability of a zinc selenide/zinc sulfide process). One would, therefore, expect that, at the boundary of the first surface, the composition is approximately 50% zinc selenide/zinc sulfide and, in the interior of the lens blank, 100% zinc sulfide in the homogeneous material. This would make the most cost effective lens.

It can further be shown that the coefficient N_{01} must be maintained to approximately $\pm 3\%$. This variation depends substantially on the imaging criteria that is established. In most processes, even those of diffusion, this is an easy coefficient to be maintained. However, variations outside of this regime can be taken into account if it is reproducible. In that circumstance, the focal length of the lens can simply be scaled appropriately. Many other design configurations exist that can be used to compensate for quadratic coefficients of the index of refraction profile.

There are a number of expected problems with a zinc selenide/zinc sulfide combination - one is the smoothness of the index of refraction profile with depth. If a ripple surface or ripple index profile is created (due to steps in the processing), one would expect a Fresnel effect to be created. If bumps are created, due to nucleation centers, one would expect the same effect as pits in the lens system. Depending upon the size of the index variation and its lateral and vertical extent, this may create an ultimate problem for this process. New analytic tools will have to be developed in order to handle these particular problems.

TABLE 1

ZnSe - ZnS SINGLE ELEMENT AXIAL GRADIENT LENSES

DIAMETER = 50 MM

FOCAL LENGTH	F#	N ₀₀	N ₀₁ (MM ⁻¹)	cv ₁ (MM ⁻¹)	cv ₂	GRADIENT DEPTH(MM)	ΔN
200 MM	4	2.430	-.211x10 ⁻²	.0059	.0025	1.84	.0039
100	2	2.430	-.390x10 ⁻²	.0126	.0061	3.93	.0154
62.5	1.25	2.430	-.122x10 ⁻¹	.0145	.0037	4.53	.0553
50	1.0	2.430	-.295x10 ⁻¹	.0147	.0009	4.59	.1355

$$N(Z) = N_{00} + N_{01}Z$$

cv₁ = CURVATURE OF FIRST SURFACE

cv₂ = CURVATURE OF SECOND SURFACE

V. REQUIREMENTS OF A RADIAL GRADIENT SINGLE ELEMENT BLANK

A number of radial gradient lenses have been designed both for the visible and for the infrared [5, 6]. In the infrared, a two element germanium based gradient index system has been designed for use in reconnaissance application [7]. It has a full field of view of 42° and is diffraction limited over nearly 0.8 of that field. The lens system is discussed elsewhere; however, this design is not currently manufacturable. Before such sophisticated lenses can be produced, it is necessary to manufacture simpler systems. The simplest lens system is the radial gradient Wood lens. In this system, the surfaces of the final lens element are plano and a radial gradient is introduced in the material with an axis of symmetry which becomes the optical element axis. The index of refraction in this system is represented by a polynomial in the radial coordinate

$$N(r) = N_{00} + N_{10}r^2 + N_{20}r^4 + \dots$$

where N_{00} is the base index of refraction (nominally 2.3 for a zinc selenide/zinc sulfide combination), N_{10} is the quadratic coefficient in the index of refraction polynomial and contributes the power of the element; and N_{20} and higher coefficients contribute to the aberration correction of the third, fifth and seventh order respectively. The power of such an element (i.e., the reciprocal of the focal length) is given by the simple relationship $-2N_{10}t$ (where t is the thickness). This assumes that the focal length is larger than the thickness of the lens. An alternate form to determine the focal length is $-r^2/2 t\Delta n$, where r is the radius of the component and Δn is the index change from center to edge due to the quadratic component. For example, for a single element lens with a diameter of 50 mm and a thickness of 10 mm. the focal length is given by the simple relationship of 31.25 divided by the index change. The f number of this system is given by the relation $-25/40\Delta n$. Thus, the index change created critically determines the focal length and f number of the system. For example, for an index change of .05 the focal length of such a system is 625 mm and the f number is 12.5. If the index change is 0.2 (the theoretical limit of the zinc selenide/zinc sulfide process) then the focal length will become 156 and the f number is approximately 3. In order to construct faster systems than this, curved surfaces will be necessary to supplement the power due to the gradient. The other alternative is to increase the thickness of the lens but this has the disadvantage of increasing the weight of the component. Some very simple examples are shown in Table 2 in which the base index and index of refraction polynomial have been described for systems in which the spherical aberration is corrected. The dispersion of the gradient has been calculated to minimize the chromatic aberration on the wavelength band of 8-12 microns. In Table 3, the equivalent parameters for a homogeneous single element lens of similar focal lengths are given. One sees that the spherical aberration of such a Wood element is essentially reduced. The Petzval field curvature, which is a difficult aberration to correct in most lens systems, is reduced proportional to the index of refraction. However, the coma is substantially larger and, thus, the addition of curved surfaces on the lens system has the advantage of not only increasing the power of the lens element but will allow the coma to be corrected.

In Table 4, the tolerances for the $f/3$ single element radial gradient component have been calculated and, in Figure 3, the ideal profile has been plotted with the error bars superimposed on it. This is only one of an infinity of solutions that could be manufactured but points the direction for future manufacturing technologies. Other solutions will lead to other focal lengths and to other f numbers. After these are manufactured, the lens then can be redesigned. It is important, however, to make a lens element of this type as it is a good representation and is relatively difficult compared to the axial gradient.

The problems associated with errors to the nucleation sites and radial gradients are identical to those of the axial gradient. Again, if the inhomogeneity variation occurs, one will see on the transmitted wavefront small perturbations.

VI. DESIGN OF AN OGIVE CORRECTOR PLATE

After a number of attempts at correcting the first order properties of an ogive surface, it has been concluded that, at least by conventional gradient techniques, this is not possible. The reason can be seen fairly simply. In the ogive system, the refracting surface is highly curved. This steep curvature is a function of the aperture. For example, rays striking near the optical axis see a very strongly refracting surface, whereas those out near the edge see, essentially, a plano window that is tilted at some very steep angle. This results in the rays being transmitted at very different angles. In the ideal situation, the light transmitted through the surface is refracted at a constant angle as a function of aperture. Of course, in the ideal situation, the ray, after refraction, would have the same angle as it did before and, thus, there would be no power introduced by it. This variation of refraction as a function of aperture is essentially a first order problem and, as we have seen by the design of an axial gradient and those of a radial gradient, this phenomenon will not be corrected by such gradients. It is, therefore, my conclusion that it is not possible, using a simple axial or radial gradient, to correct the strong aberrations introduced by an ogive surface.

Having spent considerable time analyzing this problem, it occurs to me that there is a new system that might be investigated in the future - that is, the use of Fresnel gradient index optics. In this system, the refracting power is given in the same way as a Fresnel system works - by a series of little facets but these facets are now created by index of refraction variations. This has some advantage over shadows that would normally be created and can result in strong refraction as illustrated by the standard overhead condenser lens in most overhead projectors. With this very simple system, it is possible to create strong refractions and by the use of gradient index it might be simple to manufacture with very high quality.

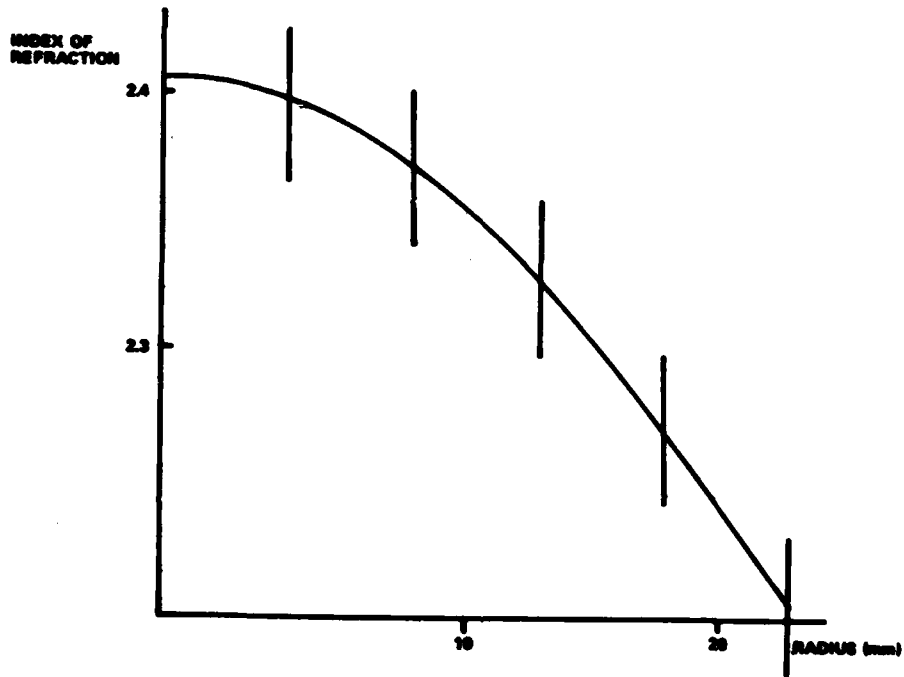


Figure 3. Index of refraction profile--f/3 wood lens.

TABLE 2

RADIAL GRADIENT WOOD LENS
DIAMETER OF LENS: 50 mm

Focal Length	N_{00}	$N_{10}(\text{mm}^{-2})$	$N_{20}(\text{mm}^{-4})$	Thickness (mm)	ΔN	Coma at 5° (mm)
200 mm	2.42	-0.25×10^{-3}	0.173×10^{-8}	10.0	0.156	-0.147
150	2.42	-0.33×10^{-3}	0.398×10^{-8}	10.0	0.206	-0.193
100	2.42	-0.50×10^{-3}	1.378×10^{-8}	10.0	0.312	-0.289
50	2.42	-1.00×10^{-3}	1.088×10^{-7}	10.0	0.625	-0.564

TABLE 3
COMPARISON OF HOMOGENEOUS SINGLET AND RADIAL GRADIENT SINGLET

$f/3, f_1 = 150 \text{ mm}$

	<u>Homogeneous</u>	<u>Wood</u>
CV_1	0.00804	
CV_2	0.00345	
TR_1	10.0	10.0
$N_{00} (= 10.6\text{mm})$	2.403	2.403
N_{10}		-0.330×10^{-3}
N_{20}		$+0.398 \times 10^{-8}$
$N_{00} (= 13.0\text{mm})$	2.385	2.385
N_{10}		-0.335×10^{-3}
N_{20}		0.398×10^{-8}
$N_{00} (= 8.2\text{mm})$	2.416	2.416
N_{10}		0.330×10^{-3}
N_{20}		0.398×10^{-8}
Field Angle	Spot Size (at 10.6mm)	
0.0°	0.430mm	0.012mm
2.5°	0.600 x 0.500mm	0.420 x 0.210mm
5.0°	1.057 x 0.700mm	0.571 x 0.466mm
	Spot Size (all wavelengths)	
0.0°	0.900mm	0.022mm
2.5°	1.080 x 0.988mm	0.601 x 0.210mm
5.0°	1.612 x 1.201mm	0.571 x 0.466mm

TABLE 4

TOLERANCES OF RADIAL GRADIENT FOR WOOD LENS

$f/3, f1 = 150 \text{ mm}$

	<u>Nominal Value</u>	<u>Error</u>	<u>% Error</u>
N_{00}	2.403	± 0.030	1.25%
N_{10}	-0.335×10^{-3}	$\pm 0.015 \times 10^{-3}$	4.5%
N_{20}	0.398×10^{-8}	$\pm 0.04 \times 10^{-3}$	10.0%

REFERENCES

1. J.J. Miceli, Infrared Gradient Index Optics: Materials, Fabrication and Testing, Ph.D. Thesis, University of Rochester, 1982.
2. N.J. Sullo, Measurements of Absolute Refractive Index Profiles in Gradient Index Materials Using Modulation Ellipsometry, M.S. Thesis, University of Rochester, 1982.
3. G.W. Johnson, Measurements of Strongly Refracting, Three Dimensional Index Distributions, Ph.D. Thesis, University of Rochester, 1979.
4. D.T. Moore, "Design of a Single Element Gradient Index Collimator," J. Opt. Soc. Am., Vol 67, No. 9, p. 1137-44 1977.
5. P.O. McLaughlin et al., "Design of a Gradient Index Binocular Objective," Proc. of the OSA 1980 International Lens Design Conference SPIE, Vol. 237, p. 369-79 (1980).
6. L.G. Atkinson et al., "Design of a Gradient Index Photographic Objective," Appl. Opt., Vol. 21, No. 6, p. 993-98 (1982).
7. D.T. Moore, Gradient Index Lens Research, Final Report, U.S. Army Missile Command, Redstone Arsenal, Alabama, Contract No. DAAH01-81-C-B042, 1982.

DISTRIBUTION

	No. of Copies
Commander, US Army Research Office	
ATTN: DRXRO-PH, Dr. R. Lontz	5
Dr. B. D. Guenther	1
P. O. Box 12211	
Research Triangle Park, NC 27709	
US Army Research and Standardization Group (Europe)	
ATTN: DRXSN-E-RX/LTC D. R. Reinhard	1
Box 65	
FPO New York 09510	
Commander, US Army Materiel Development and Readiness Command	
ATTN: Dr. James Bender	1
Dr. Gordon Bushey	1
5001 Eisenhower Avenue	
Alexandria, VA 22333	
Headquarters, Department of the Army	
Office of the DCS for Research, Development and Acquisition	
ATTN: DAMA-ARZ	1
Room 3A474, The Pentagon	
Washington, DC 20301	
OUSDRA&E	
Room 3D1079, The Pentagon	1
Washington, DC 20301	
Director	
Defense Advanced Research Projects Agency	
1400 Wilson Boulevard	1
Arlington, VA 22209	
OUSDRA&E	
ATTN: Dr. G. Gamota	
Deputy Assistant for Research (in Advanced Technology)	
Room 3D1067, The Pentagon	1
Washington, DC 20301	
Director, Defense Advanced Research Projects Agency/STO	
ATTN: Commander T. F. Wiener	1
D. W. Walsh	1
1400 Wilson Boulevard	
Arlington, VA 22209	
Commander, US Army Aviation Systems Command	
12th and Spruce Streets	
St. Louis, MO 63166	1
Director, US Army Air Mobility Research and Development Laboratory	
Ann Research Center	1
Hoffett Field, CA 94035	

Commander, US Army Electronics Research and Development Command ATTN: DRSEL-TL-T, Dr. Jacobs DELEW-E, Henry E. Sonntag Fort Monmouth, NJ 07703	 1 1
Director, US Army Night Vision Laboratory ATTN: John Johnson John Deline Peter VanAtta Fort Belvoir, VA 22060	 1 1 1
Commander US Army Picatinny Arsenal Dover, NJ 07801	 1
Commander US Army Harry Diamond Laboratories 2800 Powder Mill Road Adelphi, MD 20783	 1
Commander, US Army Foreign Science and Technology Center ATTN: W. S. Alcott Federal Office Building 220 7th Street, NE Charlottesville, VA 22901	 1
Commander US Army Training and Doctrine Command Fort Monroe, VA 22351	 1
Director, Ballistic Missile Defense Advanced Technology Center ATTN: ATC-D ATC-O ATC-R ATC-T P. O. Box 1500 Huntsville, AL 35808	 1 1 1 1
Commander, US Naval Air Systems Command Missile Guidance and Control Branch Washington, DC 20360	 1
Chief of Naval Research Department of the Navy Washington, DC 20301	 1
Commander US Naval Air Development Center Warminster, PA 18974	 1
Commander, US Naval Ocean Systems Center Code 6003 Dr. Harper Whitehouse San Diego, CA 92152	 1

Director, Naval Research Laboratory	
ATTN: Dave Ringvold	1
Code 5570, T. Gialborinzi	1
Washington, DC 20390	
Commander, Rome Air Development Center	
US Air Force	
ATTN: James Wasielewski, IRRC	1
Griffiss Air Force Base, NY 13440	
Commander, US Air Force, AFOSR/NE	
ATTN: Dr. J. A. Neff	1
Building 410	
Bolling Air Force Base	
Washington, DC 20332	
Commander	
US Air Force Avionics Laboratory	
ATTN: D. Rees	1
W. Schoonover	1
Dr. E. Champaign	1
Dr. J. Ryles	1
Gale Urban	1
David L. Flannery	1
Wright Patterson Air Force Base, OH 45433	
Commander, AFATL/LMT	
ATTN: Charles Warren	1
Eglin Air Force Base, FL 32544	
Environmental Research Institute of Michigan	
Radar and Optics Division	
ATTN: Dr. A. Kozma	1
Dr. C. C. Aleksoff	1
Juris Upatnieks	1
P. O. Box 618	
Ann Arbor, MI 41807	
IIT Research Institute	
ATTN: GACIAC	
10 West 35th Street	1
Chicago, IL 60616	
Dr. J. G. Castle	
9801 San Gabriel, NE	1
Albuquerque, NM 87111	
Dr. Vincent J. Corcoran	
2034 Freedom Lane	
Falls Church, VA 22043	1
Optical Science Consultants	
ATTN: Dr. D. L. Fried	1
P. O. Box 388	
Yerba Linda, CA 92686	

Commander, Center for Naval Analyses ATTN: Document Control 1401 Wilson Boulevard Arlington, VA 22209	1
Raytheon Company ATTN: A. V. Jelalian 528 Boston Post Road Sudbury, MA 01776	1
Dr. J. W. Goodman Information Systems Laboratory Department of Electrical Engineering Stanford University Stanford, CA 94305	1
Eric G. Johnson, Jr. National Bureau of Standards 325 S. Broadway Boulder, CO 80302	1
M. Vanderlind Battelle Columbus Labs 505 Ring Ave Columbus, OH 43201	1
Dr. Nicholas George The Institute of Optics University of Rochester Rochester, NY 14627	2
Naval Avionics Facility Indianapolis, IN 46218	1
F. B. Rotz Harris Corporation P. O. Box 37 Malbourn, FL 32901	1
Robert L. Kurtz TAI Corporation 8302 Whitesburg Dr., SE Huntsville, AL 35802	1
J. R. Vyce Itak Corporation 10 Maguire Road Lexington, MA 02173	1
Dr. David Casavant Carnegie Mellon University Hamerschlag Hall, Room 106 Pittsburg, PA 15213	1

K. G. Leib Research Department Grumman Aerospace Corporation Bethpage, NY 11714	1
Terry Turpin Department of Defense 9800 Savage Road Fort George G. Meade, MD 20755	1
Dr. Stuart A. Collins Electrical Engineering Department Ohio State University 1320 Kennear Road Columbus, OH 43212	1
Mike Scarborough, MS-19 Teledyne Brown Engineering Cummings Research Park Huntsville, AL 35807	1
Commander AFEL Hanscom Air Force Base, MD 01731	1
Dr. Arthur N. Chester Dr. Donald H. Close Thomas R. O'Meara Dr. Wilfried O. Eckhardt Hughes Research Laboratories 3011 Malibu Canyon Road Malibu, CA 90265	1 1 1 1
TRW Defense and Space Systems Group One Space Park ATTN: Dr. Peter O. Clark Redondo Beach, CA 90278	1
H. J. Caulfield Aerodyne Research, Inc. Bedford Research Park Crosby Drive Bedford, MA 01730	1
US Army Materiel Systems Analysis Activity ATTN: DRXSY-MP Aberdeen Proving Ground, MD 21005	1
US Army Night Vision Laboratory ATTN: DELNV-L, Dr. R. Buser Fort Belvoir, VA 22060	1

DRSMI-LP, Mr. Voigt	1
-O	1
-Y	1
-RN, Jerry Hagood	1
-RE, W. Pittman	1
-RD	3
-RG	1
-RR, Dr. Hartman	1
Dr. Bennett	1
Dr. Christensen	100
Dr. Duthie	1
-RPR	15
-RPT	1
 Dr. Raymond L. Taylor CVD Incorporated 35 Industrial Parkway Woburn, MA 01801	 3